Polymer Bulletin (2024) 81:14875–14902
https://doi.org/10.1007/s00289-024-05428-1

ORIGINAL PAPER

Compatibilization of poly(butylene adipate-co-terephthalate)/polylactic acid blends by gamma radiation

Fernanda Andrade Tigre da Costa[1,2] · Elizabeth Carvalho Leite Cardoso[1] · Alain Dufresne[2] · Duclerc Fernandes Parra[1]

Received: 25 April 2024 / Revised: 5 July 2024 / Accepted: 8 July 2024 /
Published online: 13 July 2024
© The Author(s), under exclusive licence to Springer-Verlag GmbH Germany, part of Springer Nature 2024

Abstract

Polylactic acid (PLA) is a widely used biopolymer and is currently produced on a global scale. However, PLA has low melt strength, which limits its application. Poly(butylene adipate-co-terephthalate) (PBAT) is a fully biodegradable polymer and one of the most attractive polymers for hardening PLA. As PLA and PBAT are immiscible, they need to be compatibilized to improve the properties of the blend. In this context, the compatibilization of PLA/PBAT blends was investigated through an irradiation process. PLA was previously irradiated, at different absorbed doses, in a cobalt-60 source to assess the compatibility of its blends with PBAT. Differential scanning calorimetry showed a reduction in the glass transition, cold crystallization and melting temperatures, and a second melting peak was observed after polymer irradiation. Also, X-ray diffraction analyses revealed a slight increase in the crystalline fraction. Thermogravimetric analysis showed that as the absorbed dose increased, the thermal stability of PLA decreased. Fourier-transform infrared spectroscopy shows bands attributed to oxidized terminations of polymer chains with carbonyls attributed to the effect of irradiation exposure. For samples irradiated above 100 kGy, an increase in tensile strength and tensile modulus can be observed as the dose increases. Rheological measurements showed a decrease in the complex viscosity of irradiated PLA with increasing absorbed dose. The surface of the polymer blend with PLA irradiated with gamma rays at 150 kGy appears to be more homogeneous according to scanning electron analysis. The polymer blend with 150 kGy irradiated PLA showed improved interaction between the components.

✉ Fernanda Andrade Tigre da Costa
fernanda.tigre@outlook.com

[1] Department of Chemistry and Environment in Nuclear and Energy Research Institute, IPEN–CNEN/SP, Cidade Universitária, Av. Prof. Lineu Prestes, 2242 – Butantã, São Paulo, SP CEP 05508-000, Brasil

[2] LGP2, CNRS, Grenoble INP, University of Grenoble Alpes, F-38000 Grenoble, France

Keywords PLA · PBAT · Compatibilization · Gamma radiation

Introduction

Polylactic acid (PLA) is a bio-based and biocompostable polymer derived from renewable resources. It is considered a viable alternative to synthetic polymers in a variety of packaging materials used for food and medical applications [1, 2]. PLA is a versatile polyester, but due to its brittleness, it is blended with other polymers to improve its performance in many applications [3]. PLA is a material characterized by high stiffness and low flexibility, and when blended with poly(butylene adipate-co-terephthalate) (PBAT), which has high processability and flexibility, the resulting blends can exhibit high performance, suitable for various applications [4].

PBAT is a biodegradable aliphatic-aromatic polyester produced from fossil sources. PBAT contains terephthalic acid, adipic acid and 1,4-butanediol monomers in its structure. The aromatic fraction (terephthalate group) presents excellent mechanical properties, while the aliphatic chains (butylene adipate group) promote its degradation [5, 6]. However, PLA/PBAT blends exhibit poor interfacial adhesion and macro-phase separation, making them immiscible [7]. Several studies evaluate the compatibility of PLA/PBAT blend with the use of different compatibilizing agents, which show satisfactory results in terms of mechanical properties [8–13].

In addition to using chemical compatibilizers, high-energy radiation, such as gamma rays and electron beams (e-beam), is gaining much interest as it can increase interfacial compatibility via interaction and recombination of macromolecular radicals [14–17]. This occurs because exposure to irradiation produces bond cleavages and free radicals that promote molecular reactions and interactions between polymer chains at the blend interfaces [18, 19]. Unlike general polyolefin macromolecular chain structures such as polypropylene and polyethylene, PLA chains tend to scission rather than branch or crosslink under high-energy irradiation due to the lack of methylene groups in the chains [20]. Figure 1 illustrates the gamma-irradiation compatibilization mechanism of PLA/PBAT blend.

In this work, the compatibility of the PLA/PBAT blend was investigated. PLA was irradiated in a multipurpose irradiator with a Cobalt-60 source at different absorbed doses, with the aim of improving interfacial compatibility through interaction and recombination of macromolecular radicals generated during radiation exposure. Mechanical tests, thermal analyses, rheological analysis, DRX and FTIR were performed to assess compatibility.

Materials and methods

Materials

PLA Ingeo® biopolymer 3D850 (density of 1.24 g/cm^3, melting temperature of 165–180 °C, melt flow rate of 7–9 g/10 min (210 °C/2.16 kg), relative viscosity of 4.0, D-lactic acid content of 0.5% [21], molecular weight of 113.4 ± 2.7 kg/mol [22])

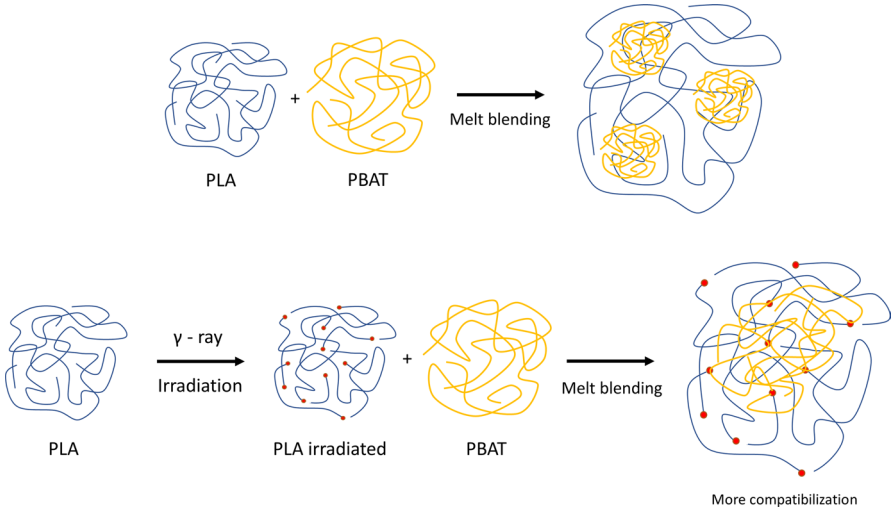

Fig. 1 Illustration of the compatibilization mechanism by gamma irradiation of PLA in PLA/PBAT blends

was purchased from NatureWorks LLC (Minnetonka, MN, USA). PBAT Ecoflex® C1200 F (density of 1.25–1.27 g/cm^3, melting temperature of 110–120 °C, melt flow rate of 2.7–4.9 g/10 min (190 °C/2.16 kg)) was obtained from BASF (Florham Park, NJ, USA). Irganox® 1010 was purchased from Easy Química LTDA (Mogi das Cruzes, SP, Brazil).

Sample preparation

PLA was previously irradiated in a multipurpose irradiator at the Radiation Technology Center (CETER) at IPEN-CNEN/SP with a source of Cobalt-60, at absorbed doses of 80, 100, 120 and 150 kGy and with an average dose rate of 3.4 kGy/h in air atmosphere and ambient temperature of 25 ± 1 °C. PLA oxidation was induced by the use of the oxidizing atmosphere during irradiation. The chosen dosage, up to 150 kGy, was carried out in a similar way to a previous study [8]. PLA/PBAT blends were prepared in different proportions (Table 1). Irganox 1010 was used as an antioxidant agent. The PLA/PBAT blends (50/50 wt%/wt%) were prepared in a Haake Rheomex model 332p co-rotational twin-screw extruder with a screw diameter of 16 mm and L/D ratio = 25 from Thermo Scientific. Extrusion was carried out with all 6 zones at a temperature of 145 °C and screw rotation speed of 80 rpm and 4 % feed. The material was cooled to room temperature and subjected to continuous granulation process in a pelletizer. To make the test specimens, the samples were then produced in an injection molding machine model III.16.AX from AX Plásticos Máquinas Técnicas Ltda., with a screw diameter of 16 mm and a length of 384 mm, dosing delay of 0.50 s, screw withdrawal speed of 56 %, screw turning speed of 95 %, cooling of 5 s, filling of 7.5 s, temperature of zones 1–4, of 110, 180, 150 and

Table 1 Composition of PLA/PBAT specimens

Nomenclature	PLA (wt%)	PBAT (wt%)	Irganox (wt%)	Absorbed dose (kGy)
PLA	100	–	–	0
PLA80	100	–	–	80
PLA100	100	–	–	100
PLA120	100	–	–	120
PLA150	100	–	–	150
PBAT	–	100	–	0
PLA/PBAT	49.85	49.85	0.3	0
PLA80/PBAT	49.85	49.85	0.3	80
PLA100/PBAT	49.85	49.85	0.3	100
PLA120/PBAT	49.85	49.85	0.3	120
PLA150/PBAT	49.85	49.85	0.3	150

30 °C, respectively, using a steel mold according to ASTM D638-14 [23] for type IV sample). No post-radiation oxidation was considered as the PLA was immediately processed at 145 °C to prepare the samples, and this was sufficient to eliminate possible residual radicals.

Characterizations

Differential scanning calorimetry (DSC)

The thermal behavior was evaluated according to ASTM D3418-12 [24] standard in three stages using Mettler Toledo equipment model DSC 822e with an atmosphere of N_2 at 20 mL/min. First, the samples were subjected to a heating rate of 10 °C/min up to 170 °C, then it was cooled to -30 °C at 10 °C/min, thus removing the thermal history from the sample. It was kept at this temperature for 5 min, and then, the samples were heated again to 170 °C at 10 °C/min. Therefore, it was possible to obtain the glass transition temperature (T_g), cold crystallization temperature (T_{cc}), cold crystallization enthalpy (ΔH_{cc}), melting temperature (T_m), melting enthalpy (ΔH_m), hot crystallization temperature (T_{hc}) and hot crystallization enthalpy (ΔH_{hc}) for each sample. The degree of crystallinity (Xc_{DSC}) of the samples was determined using Eq. 1.

$$X_{cDSC} = \frac{\Delta H_m - \Delta H_{cc}}{\Delta H^{\circ}_m} \times \frac{100}{w} \quad (1)$$

where ΔH_m is the melting enthalpy, ΔH_{cc} the cold crystallization enthalpy, ΔH°_m is the melting enthalpy for the 100% crystalline material (equivalent to 114 J/g for PBAT and 93 J/g for PLA) [25], and w is the mass fraction of PLA or PBAT in the blend.

The expected behavior of a blend of two polymers, PBAT and PLA, if they were perfectly compatible at the molecular level can be predicted by Fox Eq. (2) [26]. It is a mathematical relationship used to predict the glass transition temperature (*T*g) of such polymer blends. Fox equation considers the individual *T*gs of neat components (PBAT and PLA) and their weight fractions (*x*) in the mixture to predict a single *T*g for the blend. If PBAT and PLA were miscible, the Fox equation predicts a shift in the overall Tg of the blend relative to the individual *T*gs of PBAT and PLA. This shift in Tg reflects the influence of both polymers on the molecular mobility within the blend, ultimately affecting its physical properties.

$$\frac{1}{T_g} = \frac{x(\text{PBAT})}{T_g(\text{PBAT})} + \frac{x(\text{PLA})}{T_g(\text{PLA})} \tag{2}$$

Thermogravimetric analysis (TGA)

Thermogravimetry analyses were evaluated according to ASTM E1131-20 [27] in a Mettler Toledo thermobalance, TGA/DSC 3 + model, using heating rate of 10 °C/min to a temperature of 600 °C, with nitrogen atmosphere at 50 ml/min and open alumina crucible. Therefore, it was possible to obtain the temperature of onset decomposition, temperature of 5% of weight loss, temperature of 50% of weight loss and the residue at 600 °C (T_{onset}, $T_{5\%}$, $T_{50\%}$ and $R_{600°C}$, respectively).

Attenuated total reflection Fourier-transform infrared spectroscopy (ATR-FTIR)

The functional groups present in the samples were identified using PerkinElmer/Spectrum 65 with the UATR accessory Diamond/ZnSe crystal (3 Reflection). The scanning range was 4000–600 cm^{-1} at resolution of 4 cm^{-1} with 16 accumulations.

Tensile tests

The tensile behavior of the samples was evaluated according to ASTM D638-14 [23] standard, using universal testing equipment EMIC DL 3000, with a cross-head speed of 50 mm/min speed, a load cell of 20 kN, at a temperature of 25 ± 5 °C and relative humidity of 50% ± 5%.

X-ray diffraction analysis (XRD)

The degree of crystallinity and peak sizes were evaluated with Bruker D2 PHASER diffractometer, using CuKα monochromatic radiation (λ = 1.54184 Å), a voltage of 30 kV, and current of 10 mA. The diffraction data were obtained in the angular range 2θ = 5–60° and sweep speed of 0.05°/s. The crystallinity index (Xc_{XRD}) was measured as the ratio between the crystalline area and the total area, according to Equation 3:

$$X_{\mathrm{cXRD}} = \frac{A_C}{A_a + A_c} \times 100 \quad (3)$$

where Ac is the area of the crystalline phase, and Aa is the area of the amorphous phase. All calculations were performed using Fityk software, and the peaks were deconvoluted using Gaussian function for the amorphous halo and Voigt function for the crystalline peaks.

Rheological properties

The rheological properties of PLA and PLA/PBAT blends with and without previous irradiation were evaluated in the molten state using a rheometer Physica MCR301 from Anton-Paar with a parallel-plate (d = 25 mm) geometry. Specimens were loaded between parallel plates and melted at 170 °C. The PLA samples were 1.0 mm in thickness, while the PLA/PBAT blends samples were in 3.0 mm. The viscoelastic properties of the blends were determined by a dynamic frequency sweep test. Strain (1%) and angular frequency range (150–0.1 rad/s log) were used during testing. Complex viscosity (η*), storage modulus (G') and loss modulus (G″) in the molten state were obtained.

Electron paramagnetic resonance (EPR)

Preliminary electron paramagnetic resonance measurements were carried out to verify the presence of stable radicals formed by the interaction of ionizing radiation with the samples. In these preliminary measurements, the decay of the EPR signal with time after irradiation was not studied, nor was a dose–response curve constructed. Duplicate samples of PLA in pellet form were analyzed with doses of 0 kGy (non-irradiated), 80 kGy, 100 kGy, 120 kGy and 150 kGy. EPR measurements were performed one week after the samples were removed from the irradiator. For each measurement, 3 pellets of each sample were placed in a quartz tube. These sets were also weighed; the measured mass of each set of 3 pellets was within the range between 100 and 107 mg approximately. The analyses were performed with a Bruker EMX PLUS RPE Spectrometer operating in the X band with HS1084 High Performance cavity using 1 scan per sample, 3.510 G center field, 200 G scan window, 1 G modulation amplitude, 100 kHz modulation frequency, 20 dB gain, microwave power at 0.6325 mW, frequency microwaves (X-Band) at 9.83 GHz, without self-calibration, without rotation of the sample in the cavity. Measurements were performed at room temperature between 20 and 25 °C and relative humidity between 50 and 65%.

Scanning electron microscopy (SEM)

The morphology of irradiated and non-irradiated PLA/PBAT blends was analyzed using a FEI QUANTA-FEG 250 microscope (Thermo Fisher), with an accelerating voltage of 2.5 kV. The samples were fractured in liquid nitrogen and then coated

with gold/palladium (5 nm). Fracture images of the blends were obtained at the magnitude of × 5.0 k.

Results and discussion

Differential scanning calorimetry (DSC)

Differential scanning calorimetry was used to investigate the glass transition, crystallization and melting characteristics of PLA, PBAT and their blends and study the effect of the different absorbed doses of gamma irradiation. The thermal properties obtained during the cooling and second heating scans are summarized in Table 2. DSC curves during cooling and second heating scan are shown in Fig. 2 for PLA samples and Fig. 3 for PLA/PBAT blends. In Fig. 2, the increase in gamma irradiation led to a decrease in the glass transition temperature, cold crystallization temperature and division of the melting peak. The division of the melting peak indicates that during PLA irradiation, segments of lower molar mass were formed, and these have the characteristic of melting earlier, and as the absorbed dose was increased, the interval between the two melting peaks was increased. The decrease in glass transition and the cold crystallization temperature may be due to the chain scission that occurred as a result of the irradiation. Specifically, the decrease in Tg can be further explained by the reduction in molecular weight of PLA chains due to scission. This decrease in molecular weight is also likely responsible for the observed splitting of the melting peak, as lower-molecular-weight segments formed during irradiation tend to melt at a lower temperature compared to higher-molecular-weight chains.

Figure 3 shows that the presence of irradiated PLA appears to promote the hot crystallization of the blends suggesting an interaction between the irradiated PLA and PBAT that facilitates PLA crystallization. This is evidenced by the more intense and defined crystallization peaks for the blend when compared to the neat one. Additionally, the degree of crystallinity of the blends seems to increase slightly with higher irradiation doses of PLA, potentially due to increased interfacial interactions. This suggests that gamma irradiation, by affecting the amorphous phase, might indirectly enhance the crystallizability in the blend.

The reduction in glass transition temperature and splitting of the melting peak can still be observed in the blends due to irradiation-induced scission of PLA chains. If PBAT and PLA were miscible at the molecular level, there should be a change in glass transition temperatures [26]. However, it is important to acknowledge that the blends do not exhibit complete miscibility at the molecular level. Fox equation calculations for a hypothetical 50/50 miscible blend predict a single *T*g at 10.98 °C. However, the single detected Tg for the blend (56.92 °C) corresponds to a value close to the Tg of pure PLA (63.0 °C). This indicates the presence of distinct PLA and PBAT phases within the blend.

Despite the lack of complete miscibility, the observed decrease in *T*g of the blend upon irradiation (around 3.7 °C compared to the unirradiated blend) suggests an improvement in miscibility compared to the non-irradiated system. In

Table 2 Thermal properties of PLA, PBAT and their blends with different absorbed gamma irradiation doses obtained by DSC, and degree of crystallinity obtained by XRD

Sample	T_g[a] (°C)	T_{hc}[b] (°C)	ΔH_{hc}[c] (J/g)	T_{m1}[d] (°C)	T_{m2}[e] (°C)	ΔH_m[f] (J/g)	T_{cc}[g] (°C)	ΔH_{cc}[h] (J/g)	$Xc_{DSC\ PLA}$[i] (%)	$Xc_{DSC\ PBAT}$[j] (%)	Xc_{XRD}[k] (%)
PLA	63.0	–	–	150.5	–	0.7	60.3	0.0	0.8	–	13.8
PLA80	53.9	103.7	–	141.5	150.2	6.8	53.2	0.0	7.3	–	17.8
PLA100	54.4	117.8	–	145.2	151.2	3.9	53.8	0.0	4.2	–	9.0
PLA120	53.6	105.2	–	143.8	150.2	6.6	52.8	0.0	7.1	–	9.7
PLA150	52.9	109.8	–	143.2	149.9	4.1	53.0	0.0	4.4	–	7.6
PBAT	–	–	–	119.2	–	10.2	74.0	16.0	–	–	36.5
PLA/PBAT	56.9	115.8	7.6	148.1	–	13.2	76.6	7.5	12.3	10.0	15.9
PLA80/PBAT	54.4	102.6	14.4	142.5	151.6	14.6	77.5	7.0	16.4	13.4	20.2
PLA100/PBAT	53.1	102.6	15.2	140.0	149.4	15.9	75.7	6.8	19.7	16.0	20.2
PLA120/PBAT	52.8	101.0	14.5	140.1	149.6	14.3	80.5	7.1	15.5	12.6	17.0
PLA150/PBAT	52.8	99.3	14.8	140.7	150.0	15.5	78.1	6.8	18.6	15.2	14.9

[a]glass transition temperature; [b]hot crystallization temperature; [c]hot crystallization enthalpy; [d]first peak of melting temperature; [e]second peak of melting temperature; [f]melting enthalpy; [g]cold crystallization temperature; [h]cold crystallization enthalpy; [I]degree of crystallinity from DSC of PLA; [j]degree of crystallinity from DSC of PBAT; [k]degree of crystallinity from XRD

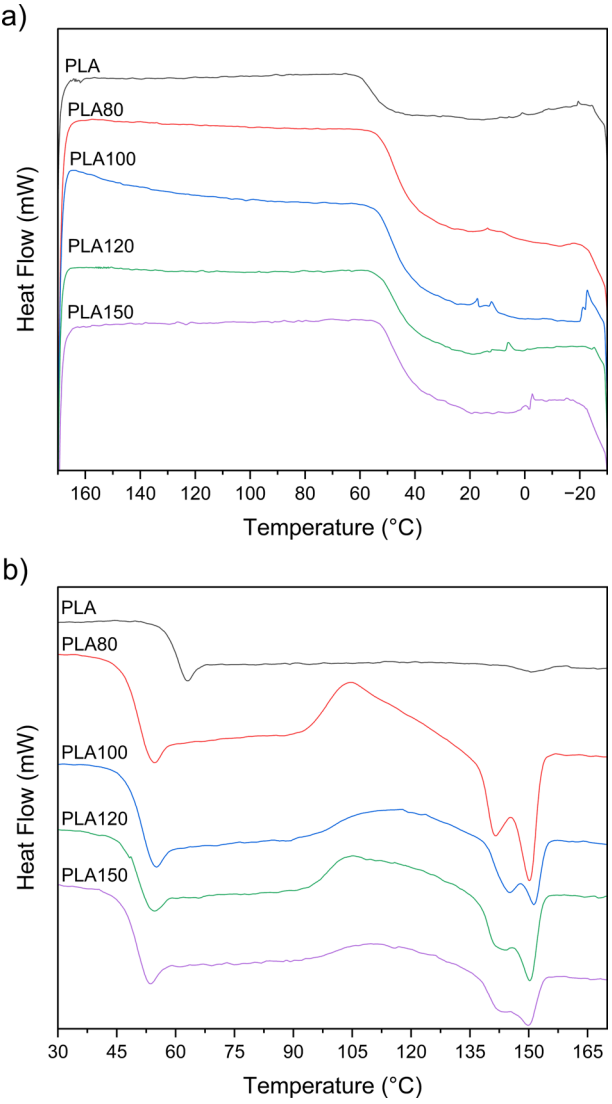

Fig. 2 DSC curves for PLA with different absorbed doses of gamma irradiation: **a** cooling from the melt; **b** second heating scan

addition to the possible decrease in *T*g due to the decrease in molecular weight during PLA irradiation, in the blend this could also be attributed to increased interfacial interactions between the irradiated PLA chains and PBAT macromolecules, leading to a more restricted mobility of the polymer chains at the interface. While not fully miscible, the irradiated PLA/PBAT blends appear to exhibit a more compatible interface compared to the non-irradiated counterparts.

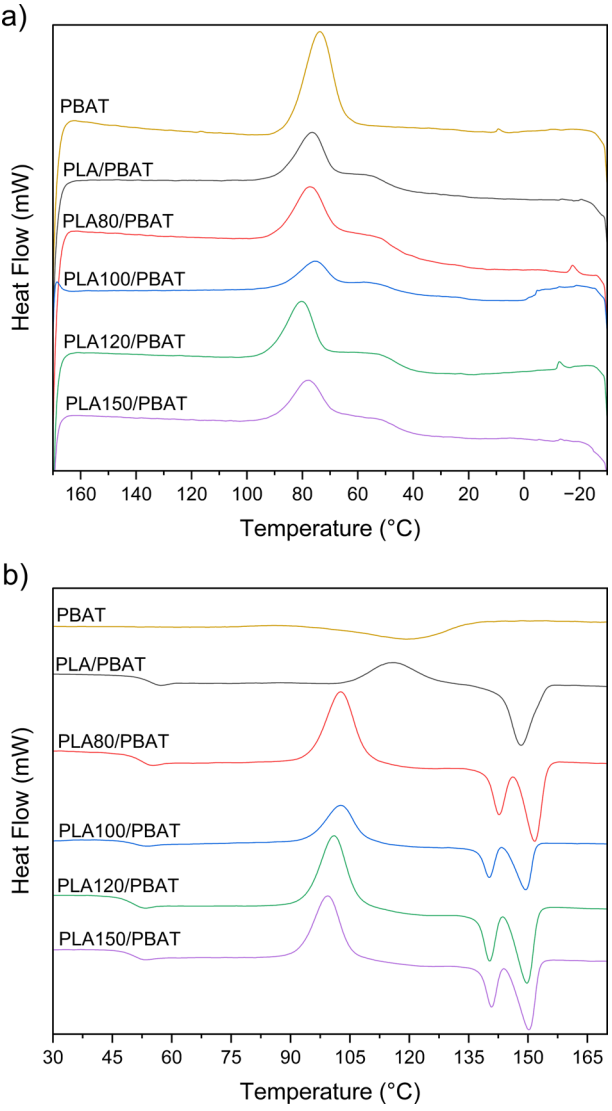

Fig. 3 DSC curves for PBAT and PLA/PBAT blends with different absorbed doses of gamma irradiation: **a** cooling from the melt; **b** second heating scan

Thermogravimetric analysis (TGA)

The thermal degradation behavior of PLA, irradiated PLA, PBAT, blends and irradiated PLA/PBAT blends is reported in Fig. 4, and data are summarized in Table 3. For PLA, increasing irradiation dose led to a slight decrease in thermal stability. The onset temperature and 5% weight loss temperature exhibited a reduction with increasing dose, reaching a maximum decrease of 4.4 °C and 5.2 °C, respectively, at

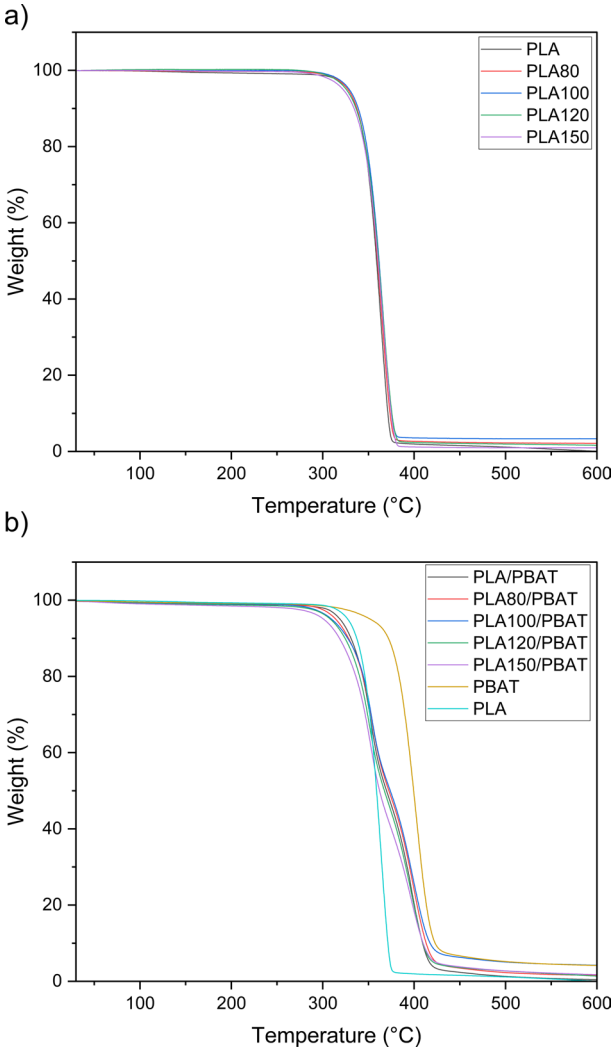

Fig. 4 TGA curves for: **a** PLA with different absorbed irradiation doses; **b** PLA, PBAT and PLA/PBAT blends with different absorbed irradiation doses

the 150 kGy dose. This suggests that gamma irradiation weakens the PLA structure, likely due to chain scission events. Interestingly, the residual mass for irradiated PLA tended to increase slightly, with the 100 kGy dose showing the most significant rise. This might be attributed to the formation of more stable, low-molecular-weight fragments during chain scission at this particular dose.

For PLA/PBAT blends, a two-step degradation process is observed, with the first stage corresponding to PLA degradation and the second stage related to PBAT degradation. Similar to neat PLA, irradiation of the PLA component within the blends resulted in a reduction of degradation temperatures for PLA (onset, 5% and 50%

Table 3 Thermogravimetric analysis data for PLA, PBAT and their blends with different absorbed gamma irradiation doses

Sample	T_{onset} (°C)	$T_{5\%}$ (°C)	$T_{50\%}$ (°C)	$R_{600°C}$ (%)
PLA	343.7	327.3	358.8	0.0
PLA80	343.3	327.5	359.8	2.1
PLA100	344.0	329.0	361.5	3.3
PLA120	341.7	325.7	361.2	1.6
PLA150	339.3	322.2	360.5	1.0
PBAT	378.9	352.2	399.5	4.2
PLA/PBAT	329.3	319.0	369.8	0.4
PLA80/PBAT	328.9	314.3	372.3	1.5
PLA100/PBAT	328.2	309.8	373.8	4.2
PLA120/PBAT	327.1	308.5	367.3	1.4
PLA150/PBAT	325.6	301.0	362.2	1.8

weight loss). Notably, the extent of this reduction increased with increasing irradiation dose. The presence of PBAT in the blends generally led to a higher average residual mass compared to irradiated PLA alone. This is likely due to the inherently higher thermal stability of PBAT. The blend containing PLA irradiated at 100 kGy (PLA100/PBAT) displayed the highest residual char content (4.23%). This observation may be linked to the potential interaction between the fragmented PLA chains (from irradiation) and the PBAT component, leading to the formation of more stable char during degradation.

Attenuated total reflection Fourier-transform infrared spectroscopy (ATR-FTIR)

FTIR spectra for neat PLA and gamma irradiated PLA with different absorbed doses are shown in Fig. 5. As expected, FTIR analysis shows that no new functionality is formed or strong chemical interactions occur as a result of gamma irradiation, since no new bands are observed. However, the spectra show that when PLA is irradiated, a slight change in the band at 3295 cm^{-1} appears, attributed to O–H stretching and its width is attributed to intermolecular and intramolecular hydrogen bonds. The bands at 2916 and 2850 cm^{-1} are assigned to the symmetrical and asymmetrical vibrational motions of the –CH groups within the PLA molecule, which the gamma irradiation strengthens the intensity of these peaks. This change can be attributed to the chain scission occurring simultaneously with oxidation reactions induced by irradiation treatment that lead to the generation of additional carboxyl and hydroxyl terminal groups in polymer chains [28], in which PLA chain promotes compatibility with PBAT in the blend. The band at 1750 cm^{-1} is also attributed to oxidized ends of the polymer chain with carbonyls, the C=O stretch. The peaks detected at 1636 cm^{-1} and 1562 cm^{-1} can be attributed to the formation of C=C double bonds [29–31]. These peaks likely originate from recombination reactions induced by gamma irradiation. During irradiation, scission of existing bonds within the polymer chains can occur. The subsequent recombination of these fragments may lead to the formation of new C=C unsaturations alongside the formation of carbonyl

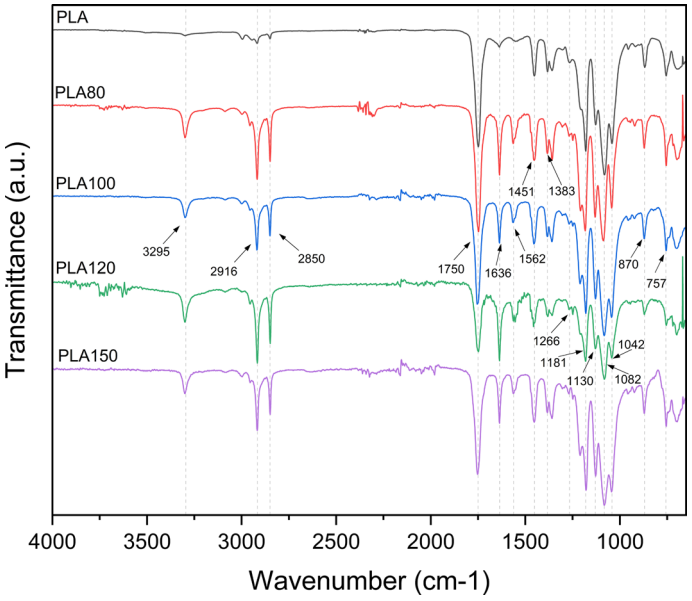

Fig. 5 FT-IR spectra for PLA with different absorbed gamma irradiation doses

groups (C = O) observed elsewhere in the spectrum. Furthermore, the increase of the irradiation dose also led to a substantial increase of these C = C double bond peaks that implies that a higher dose of gamma radiation translates to a greater extent of chain scission and subsequent C = C bond formation through recombination processes. The bands at 1451 cm^{-1} and 1383 cm^{-1} correspond to C–H bending of $–CH_3$ groups, the asymmetric and symmetric vibration, respectively. The bands at 1266, 1181, 1130, 1082 and 1042 cm^{-1} all correspond to vibrational motions of the C–O–C bond. These vibrations are complex due to the presence of various functional groups bonded to the C–O–C chain. The band at 870 cm^{-1} is related to the presence of C–O–H groups and 757 cm^{-1} is attributed as the wagging absorption of α-CH_3 of PLA.

Figure 6 shows FTIR spectra for PBAT and PLA/PBAT blends with different absorbed gamma irradiation doses. Assignment of some typical FTIR absorption bands for PLA and PBAT can be seen in Table 4. The spectra also showed a small band at 3295 cm^{-1} that is attributed to O–H stretching, bands around 2968–2858 cm^{-1} that are assigned to the symmetrical and asymmetrical stretch vibration of –CH. The band at 1711 cm^{-1} is attributed to the C = O stretch for PBAT, and for the blend, it is possible to observe that this band tends to become wider due to the C = O stretch for PLA at 1750 cm^{-1}. The band at 1636 cm^{-1} attributed to the C = C stretching vibration in PLA/PBAT blends appears to decrease in intensity with increasing irradiation dose applied to the PLA. This could be due to various factors, such as recombination reactions, in which gamma irradiation can induce chain scission, but it can also lead to recombination

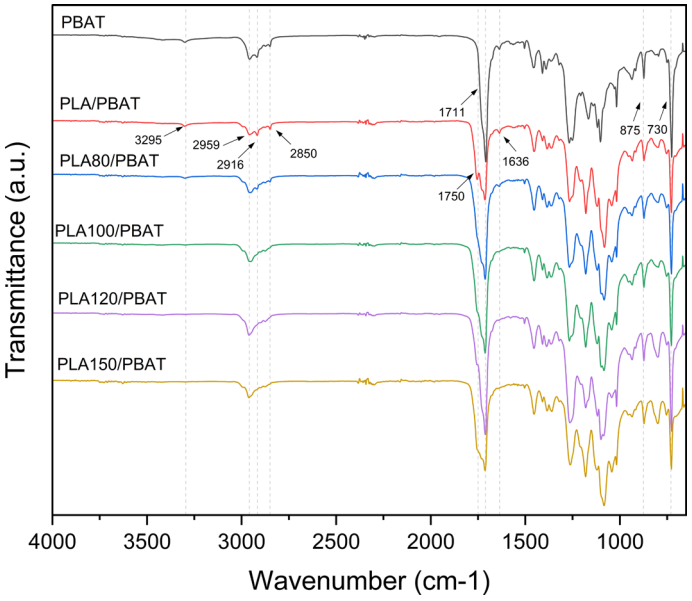

Fig. 6 FT-IR spectra for PBAT and PLA/PBAT blends with different absorbed gamma irradiation doses

Table 4 Positions and assignments of some FT-IR bands related to PLA and PBAT [8, 32–35]

Wavenumber (cm^{-1})	Assignment
3295	OH stretch
2959–2850	–CH symmetrical and asymmetrical stretch vibration in –CH3
1750	C = O stretch (PLA)
1711	C = O stretch (PBAT)
1451	–CH asymmetric vibration (PLA)
1383	–CH symmetric vibration (PLA)
1181	C–O–C asymmetric stretch (PLA)
1130	CH_3 in-plane rocking (PLA)
1082	C–O–C symmetric stretch (PLA)
1042	C–O–C stretching (PLA)
870	C–O stretching (PLA)
757	α-CH_3 vibration (PLA)
875, 730	Out-plane = C–H of benzene ring (PBAT)

reactions between the resulting fragments, leading to the formation of other functional groups (e.g., C = O carbonyls) instead of C = C double bonds. Alternatively, interactions between irradiated PLA chains and PBAT macromolecules might hinder the formation or stabilization of C = C double bonds within the blend. The

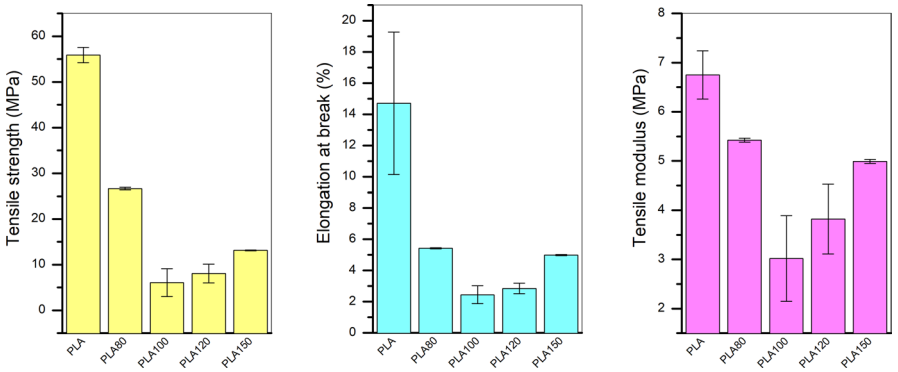

Fig. 7 Tensile mechanical properties for PLA with different absorbed gamma irradiation doses

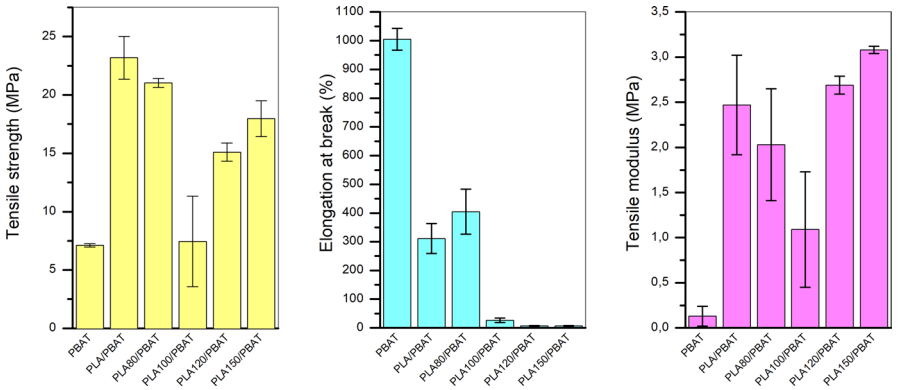

Fig. 8 Tensile mechanical properties for PBAT and PBAT/PLA blends with different absorbed gamma irradiation doses

bands at 875 and 730 cm^{-1} can be assigned as out-plane bending mode of = C–H in benzene ring of PBAT.

Tensile tests

The tensile mechanical properties, in terms of strength, elongation at break and modulus for PLA, irradiated PLA, PBAT, PBAT/PLA blends and gamma irradiated blends are shown in Figs. 7 and 8. These data are also summarized in Table 5. For PLA, we can see that as the absorbed irradiation dose increases, tensile strength, elongation at break and tensile modulus decrease. A minimum is reported for the 100 kGy dose. For higher doses, PLA120 and PLA150, a recovery of these properties is observed. The reduction in these properties is related to the chain scission effect expected from exposure to gamma irradiation, making PLA more brittle.

When adding PLA to PBAT, an increase in tensile strength and tensile modulus and a reduction in elongation at break are observed, as expected for this

Table 5 Tensile properties of PBAT/PLA blends and gamma irradiated blends

Sample	Tensile strength at yield (MPa)	Tensile modulus (MPa)	Elongation at yield (%)	Tensile stress at break (MPa)	Elongation at break (%)
PLA	55.88 ± 1.70	6.75 ± 0.49	11.62 ± 1.80	51.18 ± 2.94	14.70 ± 4.56
PLA80	26.63 ± 0.27	5.42 ± 0.04	8.80 ± 0.63	26.63 ± 0.27	5.42 ± 0.04
PLA100	6.08 ± 3.02	3.02 ± 0.87	2.43 ± 0.57	5.99 ± 3.05	2.45 ± 0.57
PLA120	8.08 ± 2.06	3.82 ± 0.71	2.84 ± 0.34	7.36 ± 3.07	2.85 ± 0.34
PLA150	13.14 ± 0.11	4.99 ± 0.04	4.3 ± 0.06	13.14 ± 0.11	4.99 ± 0.04
PBAT	7.10 ± 0.15	0.13 ± 0.11	47.51 ± 10.22	26.22 ± 1.60	1005.03 ± 38.12
PLA/PBAT	23.18 ± 1.83	2.47 ± 0.55	24.80 ± 12.03	21.91 ± 3.50	310. 98 ± 51.87
PLA80/PBAT	21.03 ± 0.39	2.03 ± 0.62	29.48 ± 13.24	19.62 ± 1.92	404.55 ± 78.69
PLA100/PBAT	7.45 ± 3.88	1.09 ± 0.64	26.64 ± 8.04	7.45 ± 3.88	26.64 ± 8.04
PLA120/PBAT	15.1 ± 0.77	2.69 ± 0.10	7.09 ± 0.68	15.08 ± 0.77	7.1 ± 0.68
PLA150/PBAT	17.96 ± 1.54	3.08 ± 0.04	7.31 ± 0.99	17.93 ± 1.49	7.33 ± 1.01

blend. The tensile strength and tensile modulus also exhibited the lowest values for PLA100/PBAT and a recovery trend when increasing the irradiation dose up to PLA150/PBAT. The improvement in tensile strength properties and decrease in elongation at break are attributed to increased compatibility between the two parent polymers in the blend. This increased compatibility results from the exposure of PLA to ionizing radiation, which induces compatibilization by free radicals, improving dispersion and adhesion of the blend phases [8, 13]. Therefore, PLA irradiated at higher doses exhibits greater compatibility with PBAT.

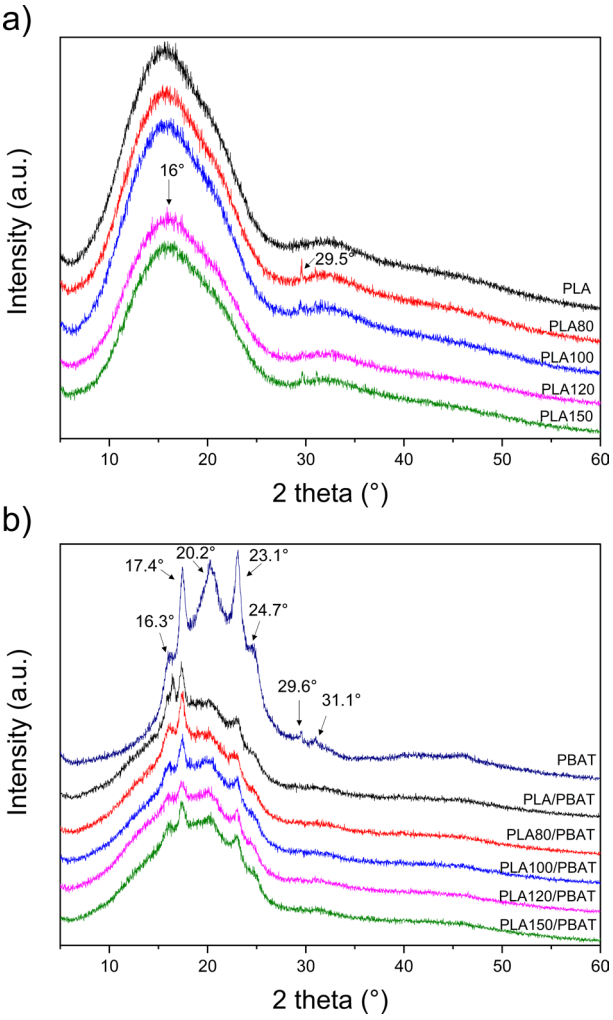

Fig. 9 XRD patterns for: **a** PLA and gamma irradiated PLA; **b** PBAT and PLA/PBAT blends with different absorbed irradiation doses

X-ray diffraction analysis (XRD)

X-ray diffraction of neat PLA, irradiated PLA, PBAT/PLA blend and gamma irradiated blends is shown in Fig. 9. PLA samples are amorphous and characterized by a broad amorphous bump located around 16°. As the absorbed gamma irradiation dose increases, a weak crystalline peak appears at 29.5°. A weak crystalline fraction can develop in irradiated samples because of the higher mobility of amorphous chains as evidenced from DSC analysis. The results are collected in Table 2. The increase in crystalline fraction was also evidenced from DSC analysis, in which the Xc value of the gamma irradiated blend tends to present a higher value than for the non-irradiated blend.

Higher doses of radiation can induce an increase in the degree of crystallinity because chain scission can also act to reduce intramolecular stress in the amorphous region, thus increasing chain mobility. The increase in mobility allows some molecules to crystallize because the crystalline state is a stable thermodynamic state [36]. These chain scissions should favor the compatibility of the blend.

Rheological behavior

It is well established that small amounts of branching, scission and crosslinking can alter the rheological properties of a polymer, and it is these reactions that can occur during the irradiation process. Scission reactions reduce the molecular weight of the polymer, resulting in lower values in the Newtonian plateau region of dynamic viscosity, while crosslinking reactions increase the molecular weight and degree of branching of the irradiated polymer [37]. The complex viscosity (η*), storage modulus (G′) and loss modulus (G″) of PLA samples and PLA/PBAT blends with different absorbed irradiation doses are compared in Figs. 10 and 11. For PLA samples (Fig. 10), the influence of gamma irradiation on PLA samples reveals that their viscosity decreases. The complex viscosity of PLA decreases sharply up to 150 kGy compared to other doses. The complex viscosity of irradiated PLA drops across the entire frequency range compared to neat PLA, while their Newtonian zone ranges are approximately the same, indicating that only a decrease in molecular weight occurs due to chain scission during gamma irradiation in the presence of oxygen.

The storage modulus and loss modulus correspond to the energy stored and consumed during the deformation process. Higher doses of gamma irradiation lead to a reduction in storage modulus lower than that of neat PLA, suggesting the occurrence of chain scission. The same behavior is observed in the reduction in loss modulus. This chain scission behavior indicates that there is a possibility of increased compatibility, since scission leaves several "openings" for new bonds, promoting compatibilization.

The current study aligns with previous investigations on the rheological properties of electron beam irradiated PLA [38]. According to the principles of linear viscoelastic theory, the observed decrease in viscosity of irradiated PLA samples suggests a transformation toward linear chain structures with narrower molecular

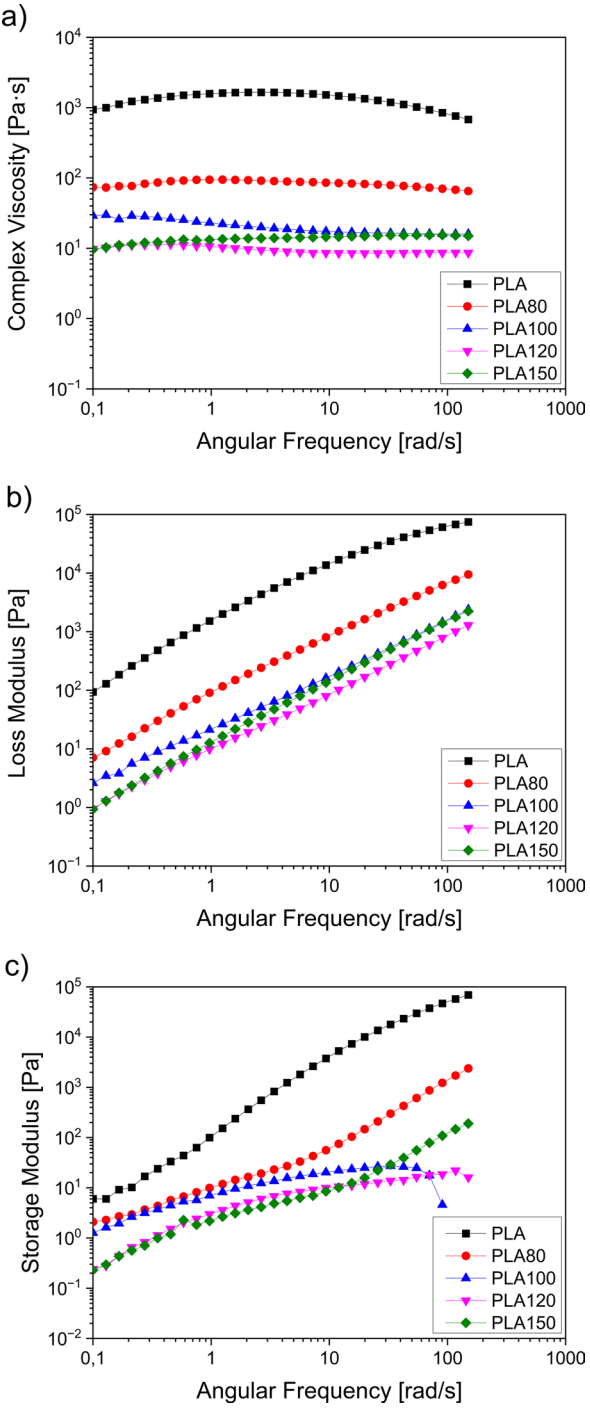

Fig. 10 Rheological properties for PLA samples with different absorbed irradiation doses: **a** complex viscosity; **b** loss Modulus; **c** storage modulus

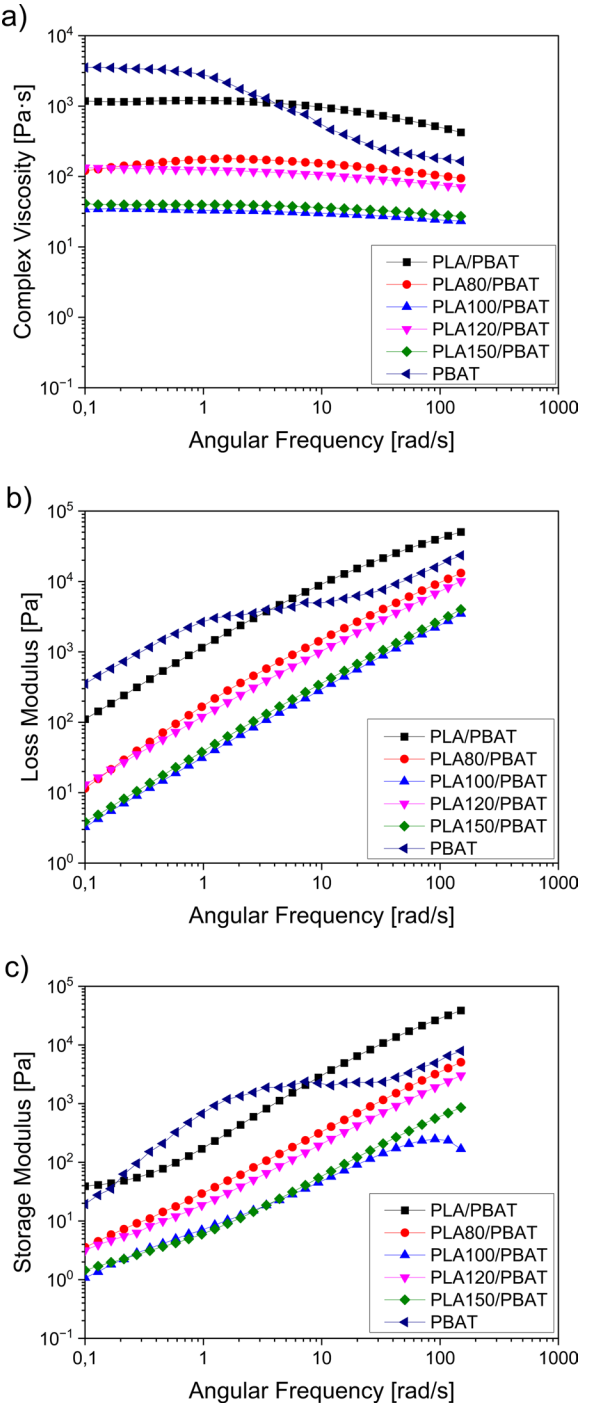

Fig. 11 Rheological properties for PBAT and PLA/PBAT blends with different absorbed irradiation doses: **a** complex viscosity; **b** loss Modulus; **c** storage modulus

weight distributions. This aligns with the established understanding that gamma irradiation primarily induces chain scission reactions within PLA. These scission events are responsible for the significant decrease in viscosity observed. However, the observed decrease in storage modulus at low oscillation frequencies suggests an additional effect beyond simple chain scission. This behavior may indicate the formation of long-chain branching (LCB) within the PLA at higher gamma irradiation doses (up to 100 kGy). LCB structures can act as physical crosslinks, potentially contributing to a network formation within the irradiated PLA. This potential for LCB formation alongside scission highlights the complexity of the chain rearrangement processes triggered by gamma irradiation in PLA.

A change in the Newtonian behavior of the storage modulus at high frequencies of PLA irradiated at 100 and slightly at 120 kGy was observed. This suggests that chain scission events, prevalent at higher irradiation doses, weaken the PLA structure. As the test frequency increases, the applied shear stress also increases. The irradiated PLA with more chain scission (100 kGy) could not withstand this higher stress, resulting in a greater reduction in storage modulus compared to the 120 kGy sample. This observation aligns with the trend of reduced mechanical properties observed more pronounced for the 100 kGy dose compared to 120 kGy, indicating a correlation between chain scission and diminished structural integrity.

For PLA/PBAT blends (Fig. 11), gamma irradiation results in a decrease in viscosity. However, all irradiated blends exhibit a similar behavior, which almost independent of the absorbed dose, only differentiating from the non-irradiated blend. The irradiated PLA/PBAT blends show more pronounced shear thinning behavior and altered Newtonian behavior in the intermediate frequency region. Therefore, when using irradiated PLA, the complex viscosity of the blends decreases. This observation may be due to the irradiation reaction that increases the interaction and entanglement capacity of PLA and PBAT chains by reacting with two chains and increasing the compatibility between PLA matrix and PBAT domains. In the PLA/PBAT blends, only the blend containing PLA irradiated at 100 kGy (PLA100) exhibited a significant decrease in viscosity and a deviation from Newtonian behavior at high frequencies in the storage modulus. This behavior mirrors the observations for neat PLA irradiated at 100 kGy, suggesting that the chain scission events and the consequent decrease in stress resistance primarily affect the PLA component within the blend at this specific irradiation dose.

Gamma irradiation appears to exert a complex influence on PLA/PBAT blends, potentially leading to two contrasting effects. Firstly, the irradiation process can promote interface modification. This is evidenced by observations in the following SEM analyses such as improved homogeneity and enhanced chain mobility within the blends, as suggested by thermal analysis results. These factors can contribute to enhanced compatibility between PLA and PBAT. Secondly, however, gamma irradiation can also induce chain scission within the polymer chains, particularly in the PLA phase. This chain scission leads to a decrease in the overall molecular weight of the irradiated material. Consequently, a reduction in viscosity can be expected. While improved chain mobility within the blend might initially suggest better mechanical properties, excessive chain scission can ultimately lead to a decrease in mechanical performance due to the loss of material strength and integrity. Therefore,

the overall impact of gamma irradiation on the properties of PLA/PBAT blends likely depends on a balance between these two opposing effects. At lower irradiation doses, the benefits of interface modification might outweigh the detrimental effects of chain scission. However, at higher doses, excessive chain scission can become dominant, resulting in a decrease in mechanical properties.

Electron paramagnetic resonance (EPR)

No EPR signal was observed in the non-irradiated sample. Figure 12 shows the EPR signals for irradiated samples. Values were normalized to 1 g of PLA. According to Babanalbandi et al. [39], the EPR signal for gamma irradiated PLA is composed of at least 3 radicals, 2 of which being more stable for measurements at room temperature. Radical (1) CH_3 is predominant, forming a quartet. Radical (2), not very expressive in the samples, is also composed of the methyl radical, forming a doublet of quartets. The distance between the main peaks was estimated to be 2.3 mT, which is the hyperfine coupling constant for the radical (1)·CH_3. For radical (2) a spectrum simulation study would be necessary, the coupling constants for the doublet and the quartet being 1 mT and 2.1 mT, respectively, different from the values reported in the literature. More studies at low temperatures can be conducted to improve the

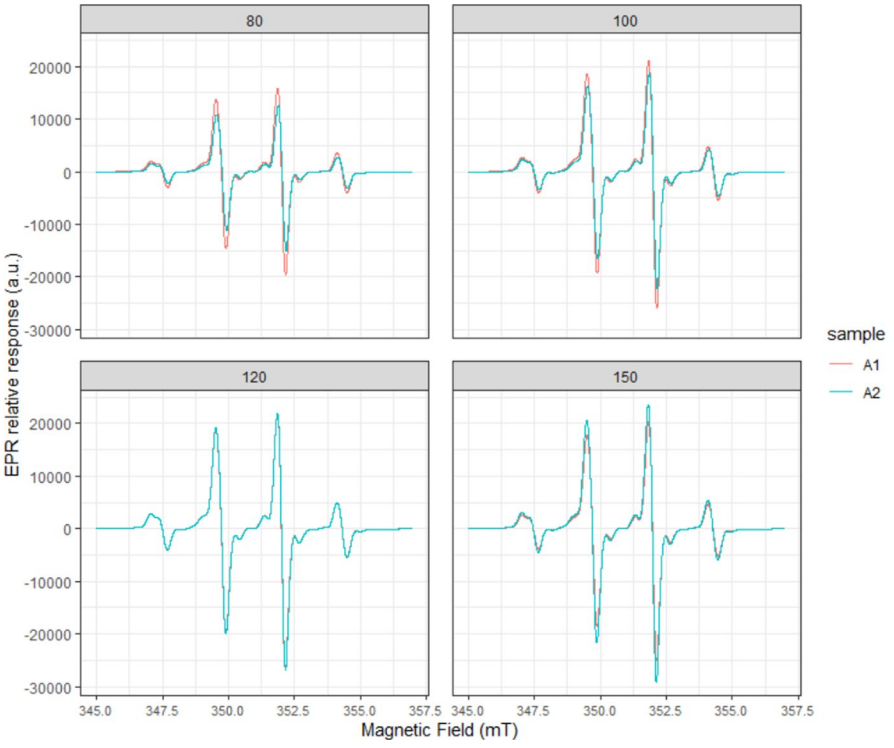

Fig. 12 EPR signal for PLA samples irradiated with Co-60

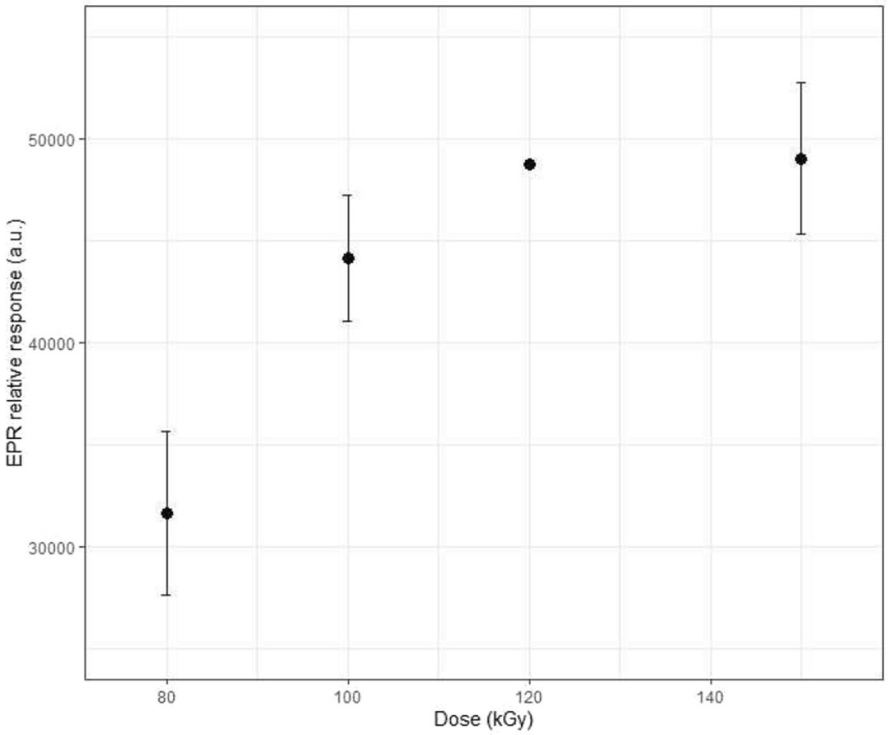

Fig. 13 Average response of the two samples for absorbed doses of 80, 100, 120 and 150 kGy

interpretation of the spectra. Regarding the generation of radicals as a result of the accumulated dose, a possible saturation for higher doses is observed in Fig. 13.

Morphological analysis

SEM micrographs of fractured surfaces of PLA/PBAT blends are shown in Fig. 14. As expected, for PLA/PBAT blend obtained from non-irradiated PLA, both domains are clearly observed. PLA and PBAT are immiscible polymers, their blends demonstrated a coarse phase separation with PLA, the continuous phase (matrix) and PBAT as the dispersed phase since PLA has higher viscosity under processing conditions than PBAT [34]. When using irradiated PLA, it is observed that the miscibility increases from PLA100kGy, for which the fracture surfaces of the blend shows a homogeneous distribution of PBAT in the PLA matrix. Gamma irradiation promotes the compatibility between PLA and PBAT, when using PLA subjected to absorbed doses higher than 100 kGy.

The increased compatibility between the two components of the blend without any compatibilizer can be induced by chemical changes due to chain scission and degradation under gamma irradiation of PLA. With the formation of methyl

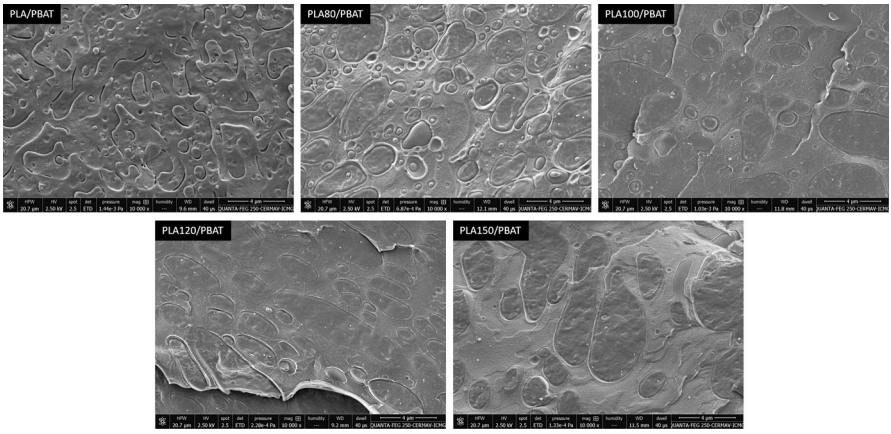

Fig. 14 SEM images showing the morphology of PLA/PBAT blends with different absorbed irradiation doses

group radicals, as shown by EPR analysis, the blending process by extrusion involving heat promotes radical combinations between PLA radicals and PBAT.

Gamma irradiation appears to promote interface modification within PLA/PBAT blends, leading to increased homogeneity and enhanced chain mobility. This is evidenced by the DSC analysis, where both cold crystallization temperature (Tcc) and hot crystallization temperature (Thc) shifted to lower values with increasing irradiation dose. This suggests faster crystallization kinetics due to the improved interfacial interactions. Furthermore, the reduction in glass transition temperature (Tg) for irradiated blends aligns with the enhanced chain mobility. However, the mechanical response exhibits a complex interplay. While increased chain mobility might suggest improved elongation at break, this behavior was only observed for the 80 kGy dose. Higher irradiation doses likely lead to excessive chain scission, resulting in brittleness and a decrease in elongation at break for blends irradiated at doses exceeding 80 kGy. These findings are similar to those reported in a previous study [11], where the addition of a compatibilizer toluenediphenyl diisocyanate (TDI) also facilitated faster crystallization and decreased Tg in PLA/PBAT blends. The study attributed this behavior to increased free volume and enhanced chain mobility due to the presence of the plasticizer Triethyl citrate (TEC). The observed reduction in Tg was even more pronounced in their compatibilized blends, suggesting a synergistic effect of both plasticization and improved compatibility between PLA and PBAT. This suggests that gamma irradiation, while not acting as a traditional compatibilizer, may create a similar effect by promoting improved interfacial interactions between PLA and PBAT.

Conclusion

In the present study, the effect of gamma irradiation of PLA under different absorbed doses of a Cobalt-60 source on the mechanical, rheological, thermal and morphological properties of PLA/PBAT blends was investigated. It was found that the mechanical properties of the samples are highly dependent on the absorbed irradiation dose, and despite the reduction in tensile strength when applying irradiation, the absorbed dose of 150 kGy shows a tendency to recover the initial strength. TGA analysis shows that as the absorbed gamma irradiation dose increases, the thermal stability of the material reduces. A small increase of the crystalline fraction was evidenced by DSC and XRD analyses. Rheological measurements showed a decrease in the complex viscosity of irradiated PLA when increasing the absorbed dose, indicating that a decrease in molecular weight occurs due to chain scission when using irradiated PLA. Therefore, PLA irradiation induces chain scission, and this scission improves the compatibility when blended with PBAT. SEM analysis reveals that gamma irradiation of PLA promotes the homogeneity of PLA/PBAT blends, indicating greater compatibility for the blends subjected to higher absorbed doses of 100 and 120 kGy. FTIR analysis shows that irradiation also contributes to more defined bands between 2750 and 3200 cm^{-1}, attributed to the chain scission occurring simultaneously with the oxidation reactions induced by radiation. In addition, C–O–C group stretching (1078–1110 cm^{-1}) indicates possible reactions of PLA radicals with PBAT macrochains. Further study of radicals decay should be carried out to broaden the discussion of the reactions between PLA radicals and PBAT.

The potential compatibilization of PLA/PBAT blends when using gamma irradiated PLA with the addition of a filler for mechanical improvement will be investigated in future studies. Currently, there is a growing intention to obtain composites with nanocellulose for greater efficiency of mechanical properties and sustainability of using cellulosic fillers. Therefore, since the modifications obtained by radiation are favorable to interfacial adhesion, the properties should be improved.

Acknowledgements To the support of CAPES-CNPq and IPEN/CNEN. LGP2 is part of the LabEx Tec 21 (Investissements d'Avenir—grant agreement n°ANR-11-LABX-0030) and of the PolyNat Carnot Institut (Investissements d'Avenir—grant agreement n°ANR-11-CARN-030-01).

Author contributions F. A. T. Costa contributed to Data curation, Writing, Original draft preparation and Editing. E. C. L. Cardoso contributed to Reviewing and Editing. A. Dufresne: Writing, Reviewing and Editing. D. F. Parra contributed to Writing, Reviewing and Editing, Validation.

Data availability No datasets were generated or analyzed during the current study.

Declarations

Conflict of interest The authors declare no competing interests.

References

1. Cheng J, Lin X, Wu X et al (2021) Preparation of a multifunctional silver nanoparticles polylactic acid food packaging film using mango peel extract. Int J Biol Macromol 188:678–688. https://doi.org/10.1016/j.ijbiomac.2021.07.161
2. Thiyagu TT, Sai Prasanna KumarGurusamy JVP et al (2023) Effect of cashew shell biomass synthesized cardanol oil green compatibilizer on flexibility, barrier, thermal, and wettability of PLA/PBAT biocomposite films. Biomass Convers Biorefin 13:11841–11851. https://doi.org/10.1007/s13399-021-01941-9
3. Su S, Kopitzky R, Tolga S, Kabasci S (2019) Polylactide (PLA) and its blends with poly(butylene succinate) (PBS): a brief review. Polymers (Basel) 11:1193. https://doi.org/10.3390/polym11071193
4. Aversa C, Barletta M, Cappiello G, Gisario A (2022) Compatibilization strategies and analysis of morphological features of poly(butylene adipate-co-terephthalate) (PBAT)/poly(lactic acid) PLA blends: a state-of-art review. Eur Polym J 173:111304. https://doi.org/10.1016/j.eurpolymj.2022.111304
5. Fu Y, Wu G, Bian X et al (2020) Biodegradation behavior of poly(butylene adipate-co-terephthalate) (PBAT), poly(lactic acid) (pla), and their blend in freshwater with sediment. Molecules 25:3946. https://doi.org/10.3390/molecules25173946
6. Kanwal A, Zhang M, Sharaf F, Li C (2022) Polymer pollution and its solutions with special emphasis on poly (butylene adipate terephthalate (PBAT)). Polym Bull 79:9303–9330. https://doi.org/10.1007/s00289-021-04065-2
7. Ding Y, Lu B, Wang P et al (2018) PLA-PBAT-PLA tri-block copolymers: effective compatibilizers for promotion of the mechanical and rheological properties of PLA/PBAT blends. Polym Degrad Stab 147:41–48. https://doi.org/10.1016/j.polymdegradstab.2017.11.012
8. Cardoso ECL, Parra DF, Scagliusi SR et al (2019) Study of bio-based foams prepared from PBAT/PLA reinforced with bio-calcium carbonate and compatibilized with gamma radiation. Use of gamma radiation techniques in peaceful applications. IntechOpen, London, pp 139–156
9. Farias da Silva JM, Soares BG (2021) Epoxidized cardanol-based prepolymer as promising biobased compatibilizing agent for PLA/PBAT blends. Polym Test 93:106889. https://doi.org/10.1016/j.polymertesting.2020.106889
10. Han Y, Shi J, Mao L et al (2020) Improvement of compatibility and mechanical performances of PLA/PBAT composites with epoxidized soybean oil as compatibilizer. Ind Eng Chem Res 59:21779–21790. https://doi.org/10.1021/acs.iecr.0c04285
11. Phetwarotai W, Phusunti N, Aht-Ong D (2019) Preparation and characteristics of poly(butylene adipate-co-terephthalate)/polylactide blend films via synergistic efficiency of plasticization and compatibilization. Chin J Polym Sci 37:68–78. https://doi.org/10.1007/s10118-019-2174-7
12. Phetwarotai W, Zawong M, Phusunti N, Aht-Ong D (2021) Toughening and thermal characteristics of plasticized polylactide and poly(butylene adipate-co-terephthalate) blend films: influence of compatibilization. Int J Biol Macromol 183:346–357. https://doi.org/10.1016/j.ijbiomac.2021.04.172
13. Wang X, Peng S, Chen H et al (2019) Mechanical properties, rheological behaviors, and phase morphologies of high-toughness PLA/PBAT blends by in-situ reactive compatibilization. Compos B Eng 173:107028. https://doi.org/10.1016/j.compositesb.2019.107028
14. de Castro DP, Sartori MDN, de Silva LG (2019) Effects of gamma radiation on the properties of the thermoplastic starch/poly (butylene adipate-co-terephthalate) blends. Mater Res 22:1–6. https://doi.org/10.1590/1980-5373-mr-2019-0072
15. Jeon JS, Han DH, Shin BY (2018) Improvements in the rheological properties, impact strength, and the biodegradability of PLA/PCL blend compatibilized by electron-beam irradiation in the presence of a reactive agent. Adv Mater Sci Eng 2018:1–8. https://doi.org/10.1155/2018/5316175
16. Kumar A, Tumu VR, Ray Chowdhury S, Ramana Reddy SVS (2019) A green physical approach to compatibilize a bio-based poly (lactic acid)/lignin blend for better mechanical, thermal and degradation properties. Int J Biol Macromol 121:588–600. https://doi.org/10.1016/j.ijbiomac.2018.10.057
17. Kumar A, Tumu VR (2019) Physicochemical properties of the electron beam irradiated bamboo powder and its bio-composites with PLA. Compos B Eng 175:107098. https://doi.org/10.1016/j.compositesb.2019.107098

18. Wang W, Zhang X, Mao Z, Zhao W (2019) Effects of gamma radiation on the impact strength of polypropylene (PP)/high density polyethylene (HDPE) blends. Results Phys 12:2169–2174. https://doi.org/10.1016/j.rinp.2019.02.020
19. Yin Y, Deng P, Zhang W, Xing Y (2018) Effect of enhanced γ-irradiation on the compatibility of polyethylene terephthalate-based basalt fiber-reinforced composites. Adv Polym Technol 37:3376–3383. https://doi.org/10.1002/adv.22121
20. Fang H, Zhang Y, Bai J et al (2013) Bimodal architecture and rheological and foaming properties for gamma-irradiated long-chain branched polylactides. RSC Adv 3:8783. https://doi.org/10.1039/c3ra40879e
21. Dechet MA, Demina A, Römling L et al (2020) Development of poly(L-lactide) (PLLA) microspheres precipitated from triacetin for application in powder bed fusion of polymers. Addit Manuf 32:100966. https://doi.org/10.1016/j.addma.2019.100966
22. Butto M, Maspoch ML, Bernal C (2023) Effect of post-drawing thermal treatment on the mechanical behavior of solid-state drawn poly(lactic acid) (PLA) filaments. Textiles 3:339–352. https://doi.org/10.3390/textiles3030023
23. American Society for Testing and Materials (2014) Standard test method for tensile properties of plastics. ASTM International, Pennsylvania, pp 1–17
24. American Society for Testing and Materials (2012) Standard test method for transition temperatures and enthalpies of fusion and crystallization of polymers by differential scanning. ASTM International, Pennsylvania, pp 1–7
25. Hernández-López M, Correa-Pacheco ZN, Bautista-Baños S et al (2019) Bio-based composite fibers from pine essential oil and PLA/PBAT polymer blend. Morphological, physicochemical, thermal and mechanical characterization. Mater Chem Phys 234:345–353. https://doi.org/10.1016/j.matchemphys.2019.01.034
26. Su S, Duhme M, Kopitzky R (2020) Uncompatibilized pbat/pla blends: manufacturability, miscibility and properties. Materials 13:1–17. https://doi.org/10.3390/ma13214897
27. American Society for Testing and Materials (2020) Standard test method for compositional analysis by thermogravimetry. ASTM International, Pennsylvania, pp 1–6
28. Alsabbagh A, Abu Saleem R, Almasri R et al (2021) Effects of gamma irradiation on 3D-printed polylactic acid (PLA) and high-density polyethylene (HDPE). Polym Bull 78:4931–4945. https://doi.org/10.1007/s00289-020-03349-3
29. Tosakul T, Suetong P, Chanthot P, Pattamaprom C (2022) Degradation of polylactic acid and polylactic acid/natural rubber blown films in aquatic environment. J Polym Res 29:242. https://doi.org/10.1007/s10965-022-03039-w
30. Chow W, Tham W, Seow P (2013) Effects of maleated-PLA compatibilizer on the properties of poly(lactic acid)/halloysite clay composites. J Thermoplast Compos Mater 26:1349–1363. https://doi.org/10.1177/0892705712439569
31. Ruf MFHM, Ahmad S, Chen RS et al (2018) Liquid natural rubber toughened poly(lactic acid) blend: effects of compatibilizer types and loadings on thermo-mechanical properties. Malays J Anal Sci 22:885–891. https://doi.org/10.17576/mjas-2018-2205-16
32. Cai Y, Lv J, Feng J (2013) Spectral characterization of four kinds of biodegradable plastics: poly (lactic acid), poly (butylenes adipate-co-terephthalate), poly (hydroxybutyrate-co-hydroxyvalerate) and poly (butylenes succinate) with FTIR and Raman spectroscopy. J Polym Environ 21:108–114. https://doi.org/10.1007/s10924-012-0534-2
33. Correa-Pacheco ZN, Black-Solís JD, Ortega-Gudiño P et al (2019) Preparation and characterization of bio-based PLA/PBAT and cinnamon essential oil polymer fibers and life-cycle assessment from hydrolytic degradation. Polymers (Basel) 12:38. https://doi.org/10.3390/polym12010038
34. Kilic NT, Can BN, Kodal M, Ozkoc G (2019) Compatibilization of PLA/PBAT blends by using epoxy-POSS. J Appl Polym Sci 136:47217. https://doi.org/10.1002/app.47217
35. Rebelo RC, Gonçalves LPC, Fonseca AC et al (2022) Increased degradation of PLA/PBAT blends with organic acids and derivatives in outdoor weathering and marine environment. Polymer (Guildf) 256:125223. https://doi.org/10.1016/j.polymer.2022.125223
36. Zhudi Z, Wenxue Y, Xinfang C (2002) Study on increase in crystallinity in γ-irradiated poly(vinylidene fluoride). Radiat Phys Chem 65:173–176. https://doi.org/10.1016/S0969-806X(02)00194-9
37. Satti AJ, Ressia JA, Cerrada ML et al (2018) Rheological analysis of irradiated crosslinkable and scissionable polymers used for medical devices under different radiation conditions. Radiat Phys Chem 144:298–303. https://doi.org/10.1016/j.radphyschem.2017.09.002

38. Wang Y, Yang L, Niu Y et al (2011) Rheological and topological characterizations of electron beam irradiation prepared long-chain branched polylactic acid. J Appl Polym Sci 122:1857–1865. https://doi.org/10.1002/app.34276
39. Babanalbandi A, Hill DJT, O'Donnell JH et al (1995) An electron spin resonance study on γ-irradiated poly(l-lactic acid) and poly(d, l-lactic acid). Polym Degrad Stab 50:297–304. https://doi.org/10.1016/0141-3910(95)00150-6

Publisher's Note Springer Nature remains neutral with regard to jurisdictional claims in published maps and institutional affiliations.

Springer Nature or its licensor (e.g. a society or other partner) holds exclusive rights to this article under a publishing agreement with the author(s) or other rightsholder(s); author self-archiving of the accepted manuscript version of this article is solely governed by the terms of such publishing agreement and applicable law.